ORIGINAL ARTICLE

Nr 2023;13 (3):476-483

Three-Dimensional Silicon Mold Analysis of the Carpal Tunnel: A Morphometric Study in Human Cadavers

Melanie Rose Dsouza[1,2], Anil K. Bhat[3], Sneha Guruprasad Kalthur[4], Samuel Allwyn Joshua[2]

[1] *Department of Basic Medical Sciences, Manipal Academy of Higher Education, Manipal, Karnataka, India*
[2] *Department of Anatomy, American University of Antigua College of Medicine, Coolidge, Antigua and Barbuda*
[3] *Department of Hand Surgery, Kasturba Medical College, Manipal Academy of Higher Education, Manipal, Karnataka, India*
[4] *Department of Anatomy, Kasturba Medical College, Manipal Academy of Higher Education, Manipal, Karnataka, India*

CORRESPONDING AUTHOR:
Anil K. Bhat
Department of Hand Surgery
Kasturba Medical College
Manipal Academy of Higher Education
Madhav Nagar, Manipal
Udupi - 576104 Karnataka, India
E-mail: anil.bhat@manipal.edu

DOI:
10.32098/mltj.03.2023.18

LEVEL OF EVIDENCE: 4

SUMMARY

Purpose. Carpal tunnel syndrome (CTS) is a common entrapment neuropathy with an incidence rate of 6%. The significance of carpal tunnel shape and dimensions in idiopathic carpal tunnel syndrome has long been debated. Recent studies have examined the accuracy of previous morphometric studies, as the reported dimensions have conflicting results. The purpose of this study was to use cadavers to determine the dimensions and shape of the carpal tunnel using a three-dimensional digitization approach.

Methods. The carpal tunnels of 35 cadavers were evacuated, and 210 silicon molds were created from 70 hands by inserting them into the soft tissue-carpeted tunnel. The mold was then scanned by a Structured Light Scanner from Steinbichler 3D scanner to obtain a three-dimensional image of the carpal tunnel, from which various carpal tunnel measures were calculated.

Results. The width, height, and cross-sectional area (CSA) of the carpal tunnel decreased significantly from proximal to distal, with a narrow CSA at the distal end. Furthermore, the ulnar side of the tunnel was observed to be significantly deeper than the radial side.

Conclusions. In this study our measured dimensions render a truncated elliptical cone-shaped carpal tunnel tapering distally. Based on our analysis, the CSA of the distal carpal tunnel may be estimated by knowledge of the proximal tunnel CSA by using the formula ($Distal_{CSA}$ = 22.137 + 0.734 ($Proximal_{CSA}$). Knowledge of the tunnel's structural architecture is important in determining the aetiology of carpal tunnel syndrome associated with variant anatomy.

KEY WORDS

Carpal tunnel syndrome; morphology; three-dimensional; morphometry; cross-sectional area; carpal tunnel shape.

INTRODUCTION

Carpal tunnel syndrome (CTS) is the most common entrapment neuropathy, affecting approximately 6% of the general population (1). Entrapment neuropathies are caused by nerve compression as it travels through constrained spaces. An increase in canal contents or a decrease in canal size raises the pressure within the tunnel, compressing the median nerve and causing CTS. Although this only affects a portion of the median nerve as it travels through the tunnel, it has significant physical, psychological, and economic consequences (2).

The causative factors of CTS are multifactorial, including risk factors such as diabetes mellitus, menopause, hypothyroidism, obesity, rheumatoid arthritis, pregnancy, injury, or trauma (3), and anatomical anomalies (4). Most cases of CTS encountered do not have an immediate evident cause. Such cases are usually termed as "idiopathic" and result usually due to a discordancy between the tunnel size and the volume of tunnel contents, thus causing an elevated pressure within the tunnel (5). Predisposing conditions correlating well with the definition of idiopathic would be pressure changes within the tunnel owing to the hypertrophied synovial membrane of the flexor tendons (6), anthropometric factors, genetic factors, advancing age as well as gender (7).

The carpal tunnel morphology is a vital factor in the etiology and management of CTS (8, 9). Among the morphological parameters, a narrow tunnel size has been underlined as a predisposing cause for idiopathic CTS, as a smaller tunnel results in a reduced space to accommodate tunnel contents (8, 10-12). The morphology of the carpal tunnel is critical in the etiology and management of CTS (8, 9). A narrow tunnel size has been highlighted as a predisposing cause for idiopathic CTS among the morphological parameters, as a smaller tunnel results in less space to accommodate tunnel contents (8, 10-12).

To attest this notion, extensive research began in the early 1980s using various techniques such as radiography (13), computed tomography (12, 14), magnetic resonance imaging (15-18), ultrasonography (19, 20), and molding (21) to study the morphological characteristics of the tunnel. The tunnel's volume, CSA, width, and length were all calculated using the methods described above. However, the reported results for volume and CSA vary greatly across studies. We believe that the inconsistencies and wide disparities in reported results are due to the researchers' disparate approaches and imaging modalities. As a result, the role of the tunnel's morphology remains unknown.

The goal of this study was to evaluate the tunnel's shape by computing its dimensions using three-dimensional scanning technology. Using the aforementioned method would allow for a near-accurate assessment of the tunnel which would also define the morphological role of the tunnel in the development of CTS.

MATERIALS AND METHODS

After seeking Institutional Ethical Clearance (this study was approved by the Kasturba Medical College and Kasturba Hospital Institutional Ethics Committee (Registration No. ECR/146/Inst/KA/2013 - Date of approval: November 17, 2015) (IEC 738/2015), 35 cadavers with a mean age of 55 were obtained from the Department of Anatomy.

Cadavers that presented any hand deformity were not included in the study. Seventy hands of the selected cadavers were dissected after placing them in anatomical position. Dissection of the tunnel was through an incision along the lateral margin of the ring finger on the palmar surface. Following this, a deeper incision was made to carefully expose the flexor retinaculum and the carpal tunnel. The median nerve and flexor tendons enclosed in their synovial sheath were emptied from the tunnel (**figure 1A**). The tunnel margins were demarcated by following the bone surfaces. The proximal border was outlined between the pisiform and scaphoid tubercle and the distal border between the hook of the hamate and trapezoidal crest (22). The proximal and distal border of the flexor retinaculum was traced.

Silicon mold was fit into the carpal tunnel to accommodate the maximum space permitted from its proximal aspect (**figure 1B**). The flexor retinaculum limits the roof of the tunnel. The retinaculum is composed of collagen fibers and having a thickness ten times more than the antebrachial fascia (13), defined the upper limit of the space available, beyond which the mold could not be fitted. In parallel, it abutted the soft tissue and the carpal bones in the tunnel floor to evaluate the actual carpal tunnel area available. After half an hour, the mold was removed and set aside to dry. This method was repeated three consecutive times on every hand to obtain three molds for each hand, and each was labelled accordingly.

The molds were then scanned by a 3-Dimensional scanner (**figure 1C**) to obtain a 3D reconstruction of the tunnel. The 3D scanner used was a Structured Light Scanner/Blue Light Scanner from Steinbichler (Germany). COMET LÆŐD is particularly well suited to measure the surfaces and profiles of objects varying from sizes as small as a few millimeters to meters long. Scanning was done by placing it in front of the scanner, followed by calibration of the machine. The area to be scanned was prepped by spraying a developer for better data extraction. The scanned mold was moved around to get as much data as possible, thereby scanned multiple times from different angles, then collated to one file and transferred

into raw data to software for post-processing. Post-processing includes deriving Iges/Step from the STL (STereoLithography) Format to CAD (Computer-Aided Design) Model for engineering applications. The STL files were then viewed in ParaView. This software is an open-source, multi-platform data analysis and visualization application to analyze three-dimensional structures. A representation of the digitized silicon mold of the carpal tunnel is shown in **figure 1D,E**.

Using the slicer tool (a filter that draws a 2-dimensional slice through a 3D data set), the 3D block was sliced from the tunnel's proximal to the distal aspect. The slices were taken at all blocks' proximal, middle, distal, and two intermediate sections (**figure 1F**). Each block was measured for volume, and each slice was measured for height, width, and CSA, respectively. The height was measured at the radial, ulnar and intermediate aspects. The widest distance represented the carpal tunnel width, and the depth was measured perpendicular to the width. The average value of the three molds of each hand was considered as the final data for the respective hand. Using SPSS 16 statistical software, a one-way analysis of variance was performed to evaluate and analyze the calculated carpal tunnel dimension differences. To compare the proximal and distal measurements, paired t was used. Using the Pearson correlation test, the relationships between proximal and distal CSAs were evaluated. Utilizing linear regression, the impact of proximal CSA on distal CSA was determined.

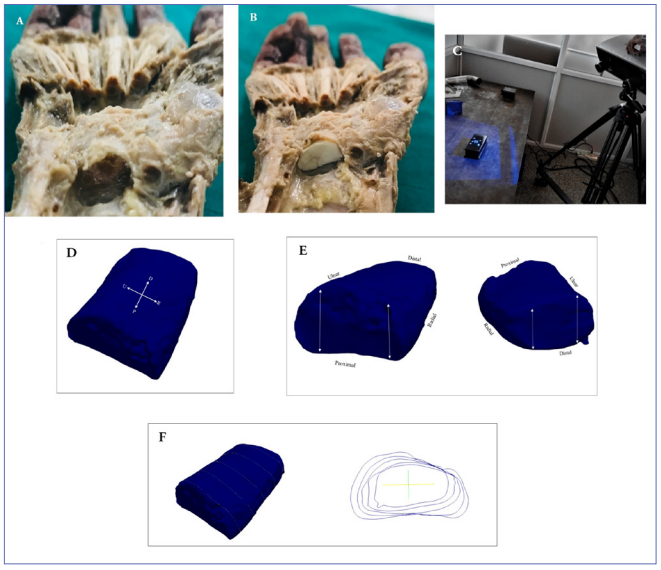

Figure 1. (A) Carpal tunnel after evacuation of contents; **(B)** Silicon mold in the evacuated carpal tunnel; **(C)** Scanning of silicon mold by 3D scanner; **(D)** Three-dimensional image of the tunnel; **(E)** Three-dimensional image of the tunnel viewed from its proximal and distal extent; **(F)** Slices taken at five intervals through the length of the tunnel.

RESULTS

The 70 cadaveric hands (n = 70) had an average carpal tunnel length of 23.5 ± 2.7 mm and volume of 3,865.5 ± 565.7 mm^3. The distal tunnel width measuring 18 ± 1.2 mm was significantly (p = 0.000) narrower in comparison with the proximal tunnel width of 19.7 ± 1.4 mm (**figure 2**). The similar modifications were observed at the tunnel's depth. The mid proximal tunnel depth was significantly larger than that of the distal end, with 10.09 ± 0.9 mm and 9.2 ± 0.9 mm respectively (p = 0.002). The depth at the proximal ulnar aspect of the tunnel was significantly (p = 0.000) greater than the radial side, measuring 9.6 ± 1.1 mm 9.0 ± 0.9 mm. Distal ulnar and radial depth were 8.35 ± 1.0 mm against 7.5 ± 1.0 mm, respectively.

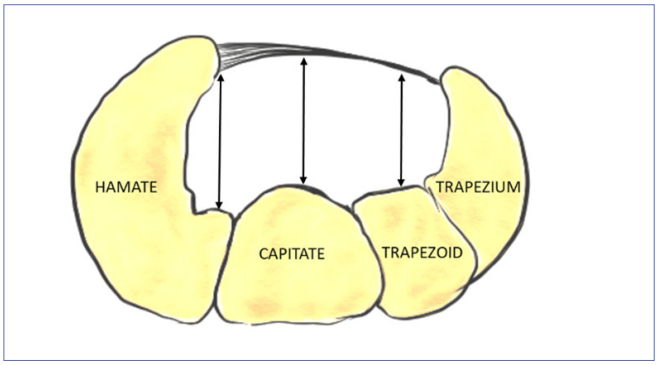

Figure 2. Impact of proximal cross-sectional area on distal cross-sectional area.

The internal dimensions of the carpal tunnel significantly correlated with the cross-sectional area (CSA). Decrease in the depth and width along the tunnel's length resulted in a significant (p = 0.000) decrease in the tunnel's CSA, which measures 182 ± 16.3 mm^2 proximally and 156 ± 16.2 mm^2 distally, rendering an elliptical truncated cone shape to the tunnel.

Paired t-test (**table I**) compares the measures between the proximal and distal in cross sectional area, ulnar height, middle height, radial height and width. From the result, it can be concluded that there exists a significant difference.

Pearson correlation test revealed a strong positive correlation between the proximal and distal cross-sectional area (r = 0.871) at $p < 0.01$ (**table II**).

Linear regression analysis proved that the proximal CSA was a significant determinant for the distal CSA ($p < 0.01$) (**table III**, **figure 3**).

From the analysis, the following regression equation can be formed to predict the impact of proximal cross-sectional on the distal cross-sectional area:

Distal cross-sectional area = 22.137 + 0.734 (Proximal cross-sectional area)

Table I. Difference between proximal and the distal.

	Proximal	Distal	t	P-value
Cross-sectional area	182.514 ± 19.547	156.057 ± 16.467	16.270	0.000
Ulnar height	9.669 ± 0.961	8.337 ± 1.082	8.631	0.000
Middle height	10.094 ± 0.973	9.411 ± 0.871	15.433	0.000
Radial height	9.023 ± 1.131	7.589 ± 1.086	9.185	0.000
Width	19.743 ± 1.486	18.069 ± 1.200	12.234	0.000

Table II. Correlation between proximal and the distal.

	Correlation
Proximal cross-sectional area and distal cross-sectional area	0.871**
Proximal ulnar height and distal ulnar height	0.607**
Proximal middle height and distal middle height	0.966**
Proximal radial height and distal radial height	0.653**
Proximal width and distal width	0.839**

**Correlation is significant at the 0.01 level (2-tailed).

Table III. Model summary for the impact of proximal cross-sectional area on distal cross-sectional area.

R	R square	Adjusted R square	Std. Error of the estimate	R square change	Change statistics			Sig. F Change
					F change	df1	df2	
0.871	0.759	0.751	8.213	0.759	103.696	1	33	0.000

	Unstandardized coefficients		Standardized coefficients		
	B	Std. Error	Beta	t	Sig.
(Constant)	22.137	13.224		1.674	0.104
Proximal cross-sectional area	0.734	0.072	0.871	10.183	0.000

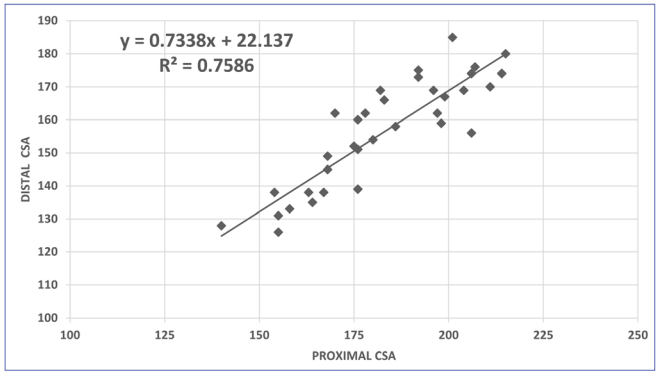

Figure 3. Diagrammatic representation of decrease in distal tunnel depth.

DISCUSSION

Our study mainly focused on the details of the structural anatomy using a cadaveric approach. The results obtained by a three-dimensional analysis indicate that the tunnel is an elliptical truncated cone-shaped passage with a wider inlet than the outlet and the ulnar depth being significantly more than the radial. Anatomical narrowing of the carpal tunnel, particularly at its outlet near the hook of the hamate, has been proposed as a factor in the development of CTS (13, 23), and our findings support this morphology.

The proximal and distal extents were determined using the bony landmarks of the tunnel margins, yielding a length of 23.5 ± 2.7 mm. Our length determination agrees well with Cobb *et al.*'s reported length of 21.7 ± 6 mm (13). Corey *et al.* (21) reported a shorter tunnel length of 12.7 ± 2.5 mm. The apparent disparity in the measures is due to different researchers' definitions of the carpal tunnel boundary. In the study by Corey *et al.* (21), the tunnel boundary was defined along the edges of the transverse carpal ligament. In contrast, we followed the bony margins to outline the tunnel's inlet and outlet. We observed a reduction in width from the inlet to the outlet, indicating that the tunnel's outlet is the segment

that is contracted. In terms of structure, it agrees with Cobb *et al.*'s findings (13), which showed that the width tapered toward the hook of the hamate. However, there is a stark difference in the computed width values when compared to ours (**table IV**). Cobb *et al.* evaluated the dimensions from radiographs after injecting the tunnel with a radio-opaque material, so the discrepancy can be attributed to a difference in technique. Their data also indicated that the tunnel's width increased beyond the hamate's hook, as they considered the base of the third metacarpal to be the tunnel's distal extent, thus visualizing the tunnel as an hourglass-shaped structure (13). In contrast, Corey *et al.* (21) cadaveric study revealed that the tunnel's width remained constant throughout its length at 19.2 ± 1.7 mm. The disparities can be explained by each individual's identification of the tunnel's extent (**table IV**).

Knowledge of the tunnel's depth is crucial for surgical planning, as it may indicate the required approach for carpal tunnel release, particularly when performing endoscopic carpal tunnel release. Elsaman *et al.* (24) used ultrasonography to measure the depth of the tunnel in the distal aspect in healthy controls and found it to be 7.91 mm. Corey *et al.* (21) reported a constant value of 8.3 ± 0.9 mm throughout the tunnel. We measured the tunnel depth from the inlet to the outlet and observed that it decreased along the length of the tunnel. The prominence of capitate along the tunnel floor (**figure 2**) and thickening of the transverse carpal ligament along the roof explains the distal decrease in tunnel depth (25). We also measured the depth along the tunnel's medial and lateral margins and discovered that the depth on the ulnar side was greater than the depth on the radial side. The greater depth can be attributed to the curvature of the hamate's hook. This measurement is critical as Alp *et al.* (26) found a strong correlation between the angle of hamate curvature and tunnel volume, emphasizing its role as a risk factor for idiopathic carpal tunnel syndrome. Surgically, this finding is consistent with the Kaplan incision line, as the ulnar aspect of the tunnel provides more room for instruments than the radial aspect of the tunnel. No prior studies have

Table IV. Cadaveric estimations of volume, cross-sectional area, width, and depth of the carpal tunnel.

	Number	Method	Volume (mm^3)	Level of section	Cross-sectional area (mm2)	Width (mm)	Depth (mm)
Current study	35	Silicon mold	3,865 ± 568	P (anatomical landmarks of inlet)	182 ± 16.3	19.7 ± 1.4	10 ± 0.9
				D (anatomical landmarks of outlet	156 ± 16.2	18 ± 1.2	9.2 ± 0.9
Corey *et al.* (2010)	10	Silicon mold	1,737 ± 542	P (proximal border of TCL)	134.9 ± 23.6	19.2 ± 1.7	8.3 ± 0.9
				D (distal border of TCL)	134.9 ± 23.6	19.2 ± 1.7	8.3 ± 0.9
Cobb *et al.* (1992)	5	MRI	3,400	P (radial styloid process)	184.7 ± 16.65	24.7 ± 1.2	-
				Hook of hamate		19.8 ± 1.2	
				D (base of third metacarpal)	155.78 ± 11.74	25.2 ± 1.5	
Gabra *et al.* (2013)	8	MRI	-	P	-	-	-
				D (hook of hamate and ridge of trapezium)	183 ± 29.7	-	-
Zong-Ming Li *et al.* (2011)	8	MRI	-	P	-	-	-
				D (hook of hamate and ridge of trapezium)	169.3 ± 29.3		

P: proximal/inlet of the tunnel; D: distal/outlet of the tunnel.

compared radial and ulnar depths. Consequently, this finding is reported for the first time.

The current study calculated the tunnel volume, which ranged from 3,300 mm^3 to 4,300 mm^3. Our volumetric data is consistent with previous studies ranging from 3,500 mm^3 to 4,500 mm^3. Corey *et al.* (21), on the other hand, reported a volume of 1,737 ± 542 mm^3. Volume is calculated from the tunnel's length, width, and height, which explains the wide disparity in reported values, as Corey *et al.* reported a smaller length, width, and depth of the tunnel as previously described. Clinically decreased tunnel volumes would increase the pressure within the tunnel thereby pinching the nerve at the narrow outlet.

The tunnel's CSA is one of the important morphological measurements as it provides a comprehensive understanding of the tunnel's anatomy. Using CSA as a metric, Dekel *et al.* (11) determined the association between tunnel stenosis and the development of idiopathic carpal tunnel syndrome via computed tomography. In addition, they reported that the narrowest portion of the tunnel was located distally in healthy subjects. Several additional authors also cited similar reports. Contrary to this, recent MRI studies have shown that the area of the hamate's hook is larger than the area of the pisiform (31). Correspondingly, Corey *et al.* found no change in the CSA and width from the inlet to the outlet in their cadaveric morphological study (19). However, we found that the tunnel gradually narrowed from the proximal to the distal extent, exhibiting a narrow CSA distally at the hook of hamate. Some studies reported CSAs as high as 275 mm^2 (11). Gabra *et al.* (32) provided a plausible explanation for this in their study. Using MRI, they calculated the carpal tunnel area by following an osseous boundary and balloon-based area. The cross-sectional value of the balloon-based area (183.9 ± 29.7 mm^2) was significantly smaller than the osseous boundary bound area (243.0 ± 40.4 mm^2). If the CSA is calculated by following the bony margin of the tunnel floor, the flexor carpi radialis tendon and soft tissue content flooring the tunnel may be included within the total cross-sectional area. **Table IV** displays the results of other reported cadaveric data. In this study we attempted to measure and subsequently identify the shape of the tunnel to almost exact precision. Consequently, we evacuated the tunnel contents, including the nerve, vessels, and tendons enclosed in their synovium. The mold was inserted abutting the soft tissue along with the carpal bones. The intercarpal ligaments over the floor were undisturbed, hence not included in the estimation of the CSA, thereby calculating the actual available carpal tunnel area.

Pearson's correlation shows that that proximal CSA is positively and significantly related to distal CSA ($r = 0.871$) at $p < 0.01$. This linear relationship implies that an increase in proximal CSA must normally be accompanied by an increase in distal CSA. Furthermore, linear regression demonstrates that the proximal cross-sectional area is a statistically significant predictor of the distal cross sectional ($p < 0.01$) and the regression model predicts the dependent variable significantly well. The impact of proximal cross-sectional area was found to be positive with $B = 0.734$ ($p < 0.01$), indicating that every unit increase in proximal cross sectional area increases distal cross sectional area by 0.734 units. This implies that the tunnel gradually narrows as we move from the inlet to the outlet. If this relationship changes and the narrowing become steeper, the pressure distally increases, predisposing to CTS. The distal carpal tunnel assessment equation may be helpful in assessing and diagnosing idiopathic CTS. Given a proximal tunnel CSA, the model provided can be used to estimate the expected distal tunnel CSA. This estimate would be useful in determining the role of structural anatomy in the onset of CTS as well as the best treatment strategy.

The present study has some limitations. It is well known that soft tissues and water content strongly influence carpal morphology in live individuals, hence, the volume of the carpal tunnel in cadavers would differ from the volume of the carpal tunnel in the living. Additionally, conditions such as hormonal variations, estrogen and diabetes, can further alter the internal dimensions of the tunnel. As cadaveric samples are standardized, we employed the same to study the shape of the tunnel precisely. Future studies involving quantitative measurements of the tunnel and its contents can be conducted utilizing this information. To comprehend the morphological differences between the sexes, these measurements must be analyzed in depth. Similarly, additional research into the differences in structural anatomy between patients and controls is required to describe the association between carpal tunnel morphology and CTS.

CONCLUSIONS

The present study used clear and easily definable anatomical landmarks and attempted to measure the available carpal tunnel space with 3D visualization. After determining the volume, length, width, height, and CSA of the carpal tunnel, we conclude that the tunnel has characteristics of an elliptical truncated cone, and that the tunnel's outlet is the narrowest segment, with the narrowing occurring gradually. The ulnar aspect of the tunnel was also found to be significantly more profound than the radial aspect. The curvature of the hamate therefore acts as a variable in contributing to the CSA and volume of the tunnel. Any alteration from the standard shape or structure of the carpal tunnel may be a predisposing factor in idiopathic carpal tunnel syndrome.

FUNDINGS

None.

DATA AVAILABILITY

Data are available under reasonable request to the corresponding author.

CONTRIBUTIONS

MRD, AKB, SGK: conceptualization, design. MRD: material preparation and data collection. SAJ: statistical analysis. MRD: writing – original draft. AKB: writing – review and editing.

ACKNOWLEDGEMENTS

The authors sincerely thank those who donated their bodies to science so that anatomical research could be performed. Results from such research can potentially increase mankind's overall knowledge that can then improve patient care. Therefore, these donors and their families deserve our highest gratitude. The authors sincerely thank Department of Anatomy Kasturba Medical College, Manipal MAHE for providing dissection lab facilities and cadavers for the study and the anatomy laboratory technicians for their assistance during this project. We thank Nandish Siddeshappa for assisting with the technical aspects of computerized 3D data analysis. We also thank Cubistry teck Solutions for assistance in 3D scanning.

CONFLICT OF INTERESTS

The authors declare that they have no conflict of interests.

REFERENCES

1. Bland JD. Carpal tunnel syndrome. BMJ. 2007;335(7615):343-6. doi: 10.1136/bmj.39282.623553.AD.
2. Foley M, Silverstein B, Polissar N. The economic burden of carpal tunnel syndrome: long-term earnings of CTS claimants in Washington State. Am J Ind Med. 2007;50(3):155-72. doi: 10.1002/ajim.20430.
3. Yunoki M, Kanda T, Suzuki K, Uneda A, Hirashita K, Yoshino K. Importance of Recognizing Carpal Tunnel Syndrome for Neurosurgeons: A Review. Neurol Med Chir (Tokyo). 2017;57(4):172-83. doi: 10.2176/nmc.ra.2016-0225.
4. Mitchell R, Chesney A, Seal S, McKnight L, Thoma A. Anatomical variations of the carpal tunnel structures. Can J Plast Surg. 2009;17(3):e3-7. Available at: https://www.ncbi.nlm.nih.gov/pmc/articles/PMC2740607/.
5. Gelberman RH, Hergenroeder PT, Hargens AR, Lundborg GN, Akeson WH. The carpal tunnel syndrome. A study of carpal canal pressures. J Bone Joint Surg Am. 1981;63(3):380-3. Available at: https://journals.lww.com/jbjsjournal/Abstract/1981/63030/The_carpal_tunnel_syndrome__A_study_of_carpal.9.aspx.
6. Schuind F, Ventura M, Pasteels JL. Idiopathic carpal tunnel syndrome: histologic study of flexor tendon synovium. J Hand Surg Am. 1990;15(3):497-503. doi: 10.1016/0363-5023(90)90070-8.
7. Lozano-Calderón S, Anthony S, Ring D. The quality and strength of evidence for etiology: example of carpal tunnel syndrome. J Hand Surg Am. 2008;33(4):525-38. doi: 10.1016/j.jhsa.2008.01.004.
8. Bekkelund SI, Pierre-Jerome C. Does carpal canal stenosis predict outcome in women with carpal tunnel syndrome? Acta Neurol Scand. 2003;107(2):102-5. doi: 10.1034/j.1600-0404.2003.02093.x.
9. Kato T, Kuroshima N, Okutsu I, Ninomiya S. Effects of endoscopic release of the transverse carpal ligament on carpal canal volume. J Hand Surg Am. 1994;19(3):416-9. doi: 10.1016/0363-5023(94)90055-8.
10. Cobb TK, Bond JR, Cooney WP, Metcalf BJ. Assessment of the ratio of carpal contents to carpal tunnel volume in patients with carpal tunnel syndrome: a preliminary report. J Hand Surg Am. 1997;22(4):635-9. doi: 10.1016/s0363-5023(97)80120-7.
11. Dekel S, Papaioannou T, Rushworth G, Coates R. Idiopathic carpal tunnel syndrome caused by carpal stenosis. Br Med J. 1980;280(6227):1297-9. doi: 10.1136/bmj.280.6227.1297.
12. Bleecker ML, Bohlman M, Moreland R, Tipton A. Carpal tunnel syndrome: role of carpal canal size. Neurology. 1985;35(11):1599-604. doi: 10.1212/wnl.35.11.1599.
13. Cobb TK, Dalley BK, Posteraro RH, Lewis RC. Anatomy of the flexor retinaculum. J Hand Surg Am. 1993;18(1):91-9. doi: 10.1016/0363-5023(93)90251-W.
14. Jessurun W, Hillen B, Zonneveld F, Huffstadt AJ, Beks JW, Overbeek W. Anatomical relations in the carpal tunnel: a computed tomographic study. J Hand Surg Br. 1987;12(1):64-7. doi: 10.1016/0266-7681_87_90061-1.
15. Richman JA, Gelberman RH, Rydevik BL, Gylys-Morin VM, Hajek PC, Sartoris DJ. Carpal tunnel volume determination by magnetic resonance imaging three-dimensional reconstruction. J Hand Surg Am. 1987;12(5 Pt 1):712-7. doi: 10.1016/s0363-5023(87)80054-0.
16. Mogk JP, Keir PJ. Evaluation of the carpal tunnel based on 3-D reconstruction from MRI. J Biomech. 2007;40(10):2222-9. doi: 10.1016/j.jbiomech.2006.10.033.
17. Mesgarzadeh M, Schneck CD, Bonakdarpour A. Carpal tunnel: MR imaging. Part I. Normal anatomy. Radiology. 1989;171(3):743-8. doi: 10.1148/radiology.171.3.2717746.
18. Mesgarzadeh M, Schneck CD, Bonakdarpour A, Mitra A, Conaway D. Carpal tunnel: MR imaging. Part II. Carpal tunnel syndrome. Radiology. 1989;171(3):749-54. doi: 10.1148/radiology.171.3.2541464.
19. Kamolz LP, Beck H, Haslik W, et al. Carpal tunnel syndrome: a question of hand and wrist configurations? J Hand Surg Br. 2004;29(4):321-4. doi: 10.1016/j.jhsb.2003.09.010.
20. Altinok T, Karakas HM. Ultrasonographic evaluation of age-related changes in bowing of the flexor retinaculum. Surg Radiol Anat. 2004;26(6):501-3. doi: 10.1007/s00276-004-0268-5.
21. Pacek CA, Tang J, Goitz RJ, Kaufmann RA, Li ZM. Morphological analysis of the carpal tunnel. Hand (N Y). 2010;5(1):77-81. doi: 10.1007/s11552-009-9220-9.
22. Gray H, Standring S. Gray's anatomy: the anatomical basis of clinical practice. Churchill Livingstone; 2005.

23. Robbins H. Anatomical study of the median nerve in the carpal tunnel and etiologies of the carpal-tunnel syndrome. JBJS. 1963 1;45(5):953-66. Available at: https://journals.lww.com/jbjsjournal/Abstract/1963/45050/Anatomical_Study_of_the_Median_Nerve_in_the_Carpal.5.aspx.
24. Elsaman AM, Thabit MN, Radwan AR, Ohrndorf S. Idiopathic Carpal Tunnel Syndrome: Evaluation of the Depth of the Carpal Tunnel by Ultrasonography. Ultrasound Med Biol. 2015;41(11):2827-35. doi: 10.1016/j.ultrasmedbio.2015.06.018.
25. Rotman MB, Donovan JP. Practical anatomy of the carpal tunnel. Hand Clin. 2002;18(2):219-30. doi: 10.1016/s0749-0712(01)00003-8.
26. Alp NB, Kaleli T, Kalay OC, et al. The Effect of Hamatum Curvature Angle on Carpal Tunnel Volumetry: A Mathematical Simulation Model. Comput Math Methods Med. 2020;2020:7582181. doi: 10.1155/2020/7582181.
27. Allmann KH, Horch R, Uhl M, et al. MR imaging of the carpal tunnel. Eur J Radiol. 1997;25(2):141-5. doi: 10.1016/s0720-048x(96)01038-8.
28. Skie M, Zeiss J, Ebraheim NA, Jackson WT. Carpal tunnel changes and median nerve compression during wrist flexion and extension seen by magnetic resonance imaging. J Hand Surg Am. 1990;15(6):934-9. doi: 10.1016/0363-5023(90)90019-n.
29. Cobb TK, Dalley BK, Posteraro RH, Lewis RC. Establishment of carpal contents/canal ratio by means of magnetic resonance imaging. J Hand Surg Am. 1992;17(5):843-9. doi: 10.1016/0363-5023(92)90454-w.
30. Yoshioka S, Okuda Y, Tamai K, Hirasawa Y, Koda Y. Changes in carpal tunnel shape during wrist joint motion. MRI evaluation of normal volunteers. J Hand Surg Br. 1993;18(5):620-3. doi: 10.1016/0266-7681(93)90018-b.
31. Bower JA, Stanisz GJ, Keir PJ. An MRI evaluation of carpal tunnel dimensions in healthy wrists: Implications for carpal tunnel syndrome. Clin Biomech (Bristol, Avon). 2006;21(8):816-25. doi: 10.1016/j.clinbiomech.2006.04.008.
32. Gabra JN, Li ZM. Carpal Tunnel Cross-Sectional Area Affected by Soft Tissues Abutting the Carpal Bones. J Wrist Surg. 2013;2(102):73-8. doi: 10.1055/s-0032-1329593.